Updating Properties of Nonlinear Dynamical Systems with Uncertain Input

Ka-Veng Yuen[1] and James L. Beck[2]

Abstract: A spectral density approach for the identification of linear systems is extended to nonlinear dynamical systems using only incomplete noisy response measurements. A stochastic model is used for the uncertain input and a Bayesian probabilistic approach is used to quantify the uncertainties in the model parameters. The proposed spectral-based approach utilizes important statistical properties of the Fast Fourier Transform and their robustness with respect to the probability distribution of the response signal in order to calculate the updated probability density function for the parameters of a nonlinear model conditional on the measured response. This probabilistic approach is well suited for the identification of nonlinear systems and does not require huge amounts of dynamic data. The formulation is first presented for single-degree-of-freedom systems and then for multiple-degree-of freedom systems. Examples using simulated data for a Duffing oscillator, an elastoplastic system and a four-story inelastic structure are presented to illustrate the proposed approach.

DOI: 10.1061/(ASCE)0733-9399(2003)129:1(9)

CE Database keywords: Bayesian analysis; Nonlinear systems; Spectral density function.

Introduction

The problem of system identification of structural or mechanical systems using dynamic data has received much attention over the years because of its importance in response prediction, control and health monitoring (Natke and Yao 1988; Housner et al. 1997). However, the results of system identification studies are usually restricted to the ''optimal'' estimates of the model parameters, whereas there is additional information related to the uncertainty associated with these estimates which is very important. For example, how precisely are the values of the individual parameters pinned down by the measurements made on the system? Probability distributions may be used to describe this uncertainty quantitatively and so avoid misleading results (Beck 1990; Beck and Katafygiotis 1998). Also, if the identification results are used for damage detection, this probability distribution for the identified model parameters may be used to compute the probability of damage (Vanik et al. 2000).

An important special case of system identification is where the input is unknown so only response measurements are available. In particular, this is the case in ambient vibrations surveys where the naturally occurring vibrations of a structure (due to wind, traffic, microtremors and structural operations) are measured (Gersch et al. 1976; Beck et al. 1994). The uncertain input excitation is usually modeled as a broadband stationary stochastic process such as white noise. Usually a linear structural model is then employed to estimate the parameters of the contributing modes of vibration.

System identification using linear models is appropriate for the small-amplitude ambient vibrations of a structure that are continuously occurring. There is, however, a number of cases in recent years where the strong-motion response of a structure has been recorded but not the corresponding seismic excitation. In some cases, this is because of inadequate instrumentation of the structure and, in other cases, it is because the free-field or base sensors malfunctioned during the earthquake. For example, the seismic response was recorded in several steel-frame buildings in Los Angeles which were damaged by the 1994 Northridge earthquake, but an analysis of these important records has been hampered by the fact that the input (base motions) were not recorded and also because of the strong nonlinear response.

A literature search reveals relatively few papers that deal with system identification using nonlinear models and measurements of only the system response (Hoshiya and Saito 1984; Loh and Tsaur 1988; Roberts et al. 1995; Zeldin and Spanos 1998). In this paper, this subject is tackled using a stochastic model for the uncertain input and a Bayesian probabilistic approach to quantify the uncertainties in the model parameters. This Bayesian probabilistic system identification framework was first presented for the case of measured input (Beck 1990; Beck and Katafygiotis 1998; Katafygiotis et al. 1998; Yuen and Katafygiotis 2002) and it has been recently extended to the case of unknown input and linear structural models (Yuen 1999; Yuen and Katafygiotis 2001; Katafygiotis and Yuen 2001; Yuen et al. 2002). The proposed approach is spectral-based and utilizes important statistical properties of the fast Fourier transform (FFT) and their robustness with respect to the probability distribution of the response signal, e.g., regardless of the stationary stochastic model for this signal, its FFT is approximately Gaussian distributed. The method allows for the direct calculation of the probability density function (PDF) for the parameters of a nonlinear model conditional on the measured response. The formulation is first presented for single-degree-of-freedom (SDOF) systems and then for multiple-degree-

[1]PhD Candidate, Division of Engineering and Applied Sciences, California Institute of Technology, Pasadena, CA 91125.

[2]Professor, Division of Engineering and Applied Science, California Institute of Technology, Pasadena, CA 91125. E-mail: jimbeck@caltech.edu

Note. Associate Editor: Roger G. Ghanem. Discussion open until June 1, 2003. Separate discussions must be submitted for individual papers. To extend the closing date by one month, a written request must be filed with the ASCE Managing Editor. The manuscript for this paper was submitted for review and possible publication on October 8, 2001; approved on May 20, 2002. This paper is part of the ***Journal of Engineering Mechanics***, Vol. 129, No. 1, January 1, 2003. ©ASCE, ISSN 0733-9399/2003/1-9–20/$18.00.

of-freedom (MDDF) systems. Examples using simulated data for a Duffing oscillator, an elastoplastic system, and a four-story inelastic structure are presented to illustrate the proposed approach.

Single-Degree-of-Freedom Systems

Bayesian System Identification Formulation

Consider a structural or mechanical system whose displacement response x is modeled using a SDOF oscillator with equation of motion:

$$m\ddot{x}+f_s(x,\dot{x};\boldsymbol{\theta}_s)=f(t) \tag{1}$$

where m, $\boldsymbol{\theta}_s$ and $f_s(x,\dot{x};\boldsymbol{\theta}_s)$ are the mass (assumed known), the model parameters, and the nonlinear restoring force of the oscillator, respectively. Furthermore, the uncertain system input is modeled as a zero-mean stationary Gaussian random process f with power spectral density function $S_f(\omega;\boldsymbol{\theta}_f)$, where $\boldsymbol{\theta}_f$ denotes the parameters of the stochastic process model for the excitation $f(t)$. The observed system response y is assumed to be stationary and is modeled by

$$y(t)=x(t)+\eta(t) \tag{2}$$

where the prediction error η accounts for modeling errors (differences between the system behavior and the model) as well as measurement noise. The uncertain prediction error is modeled as independent zero-mean Gaussian white noise, so

$$S_y(\omega)=S_x(\omega)+S_{\eta 0} \tag{3}$$

where S_y, S_x, and $S_{\eta 0}$ are the power spectral densities for the system response, model response and the prediction error. The spectral density function S_x, or the corresponding autocorrelation function R_x, can be approximated by equivalent linearization methods (Roberts and Spanos 1990; Lutes and Sarkani 1997) or by simulations.

Let $\hat{\mathbf{Y}}_N=[\hat{y}(0),\hat{y}(1),\ldots,\hat{y}(N-1)]^T$ denote a vector consisting of observed response data sampled at a time step Δt, where $\hat{y}(n)\equiv\hat{y}(n\Delta t)$, $n=0,\ldots,N-1$. Herein, we are concerned with updating the uncertainty regarding the values of the model parameters $\mathbf{a}=[\boldsymbol{\theta}_s^T,\boldsymbol{\theta}_f^T,\sigma_{\eta 0}]^T$ by using the data $\hat{\mathbf{Y}}_N$ where $\sigma_{\eta 0}^2=2\pi S_{\eta 0}/\Delta t$. From Bayes' theorem, the updated (posterior) PDF of the model parameters $\mathbf{a}$ given the data $\hat{\mathbf{Y}}_N$ is

$$p(\mathbf{a}|\hat{\mathbf{Y}}_N)=c_1 p(\mathbf{a})p(\hat{\mathbf{Y}}_N|\mathbf{a}) \tag{4}$$

where c_1 = a normalizing constant and $p(\mathbf{a})$ = the prior PDF describing our initial belief about the uncertain parameter values. Note that $p(\mathbf{a}|\hat{\mathbf{Y}}_N)$ can be used to give the relative plausibility between two values of a based on measured data $\hat{\mathbf{Y}}_N$ which does not depend on the normalizing constant c_1. Also, the most probable value of $\mathbf{a}$, denoted by $\hat{\mathbf{a}}$ (the optimal parameter values), is given by maximizing $p(\mathbf{a})p(\hat{\mathbf{Y}}_N|\mathbf{a})$. For large N, the likelihood $p(\hat{\mathbf{Y}}_N|\mathbf{a})$ is the dominant factor on the right-hand side of Eq. (4) and so $\hat{\mathbf{a}}$ is insensitive to the choice of the prior PDF $p(\mathbf{a})$ as long as the class of models is ''globally identifiable'' based on the data $\hat{\mathbf{Y}}_N$ (Beck and Katafygiotis 1998). In this case, a locally noninformative prior (Box and Tiao 1973) can be chosen; in effect, $p(\mathbf{a})$ may be absorbed into the normalizing constant c_1 in Eq. (4).

A difficulty with implementing this approach is establishing the joint distribution $p(\hat{\mathbf{Y}}_N|\mathbf{a})$ for the response of the nonlinear system. Note that the response is not Gaussian distributed but the FFT of the response is (at least approximately). We utilize this property to obtain a response PDF in the next section.

Bayesian Spectral Density Approach

Consider the stationary stochastic process $y(t)$ and the discrete estimator of its power spectral density $S_y(\omega)$:

$$S_{y,N}(\omega_k)=\frac{\Delta t}{2\pi N}\left|\sum_{n=0}^{N-1}\exp(-i\omega_k n\Delta t)y(n)\right|^2 \tag{5}$$

where $\omega_k=k\Delta\omega$, $k=0,\ldots,N_1-1$ with $N_1=\mathrm{INT}(N/2)$, $\Delta\omega=2\pi/T$, and $T=N\Delta t$. Here, INT denotes integer part. It can be shown that the estimator $S_{y,N}(\omega_k)$ is asymptotically unbiased, that is,

$$\lim_{N\to\infty}E[S_{y,N}(\omega_k)]=S_y(\omega_k) \tag{6}$$

where $E[.]$ denotes expectation (Yaglom 1987). However, for finite N, this estimator is biased. Calculating the expectation of the estimator in Eq. (5) yields

$$E[S_{y,N}(\omega_k)]=\frac{\Delta t}{2\pi N}\sum_{n=0}^{N-1}\gamma_n R_x(n\Delta t)\cos(n\omega_k\Delta t)+S_{\eta o}. \tag{7}$$

where R_x = the autocorrelation function of the response $x(t)$ and γ_n is given by

$$\gamma_n=N,\quad n=0$$
$$\gamma_n=2(N-n),\quad n\geqslant 1 \tag{8}$$

Note that the right-hand side of Eq. (7) can be calculated using the FFT of the sequence $\gamma_n R_x(n\Delta t)$, $n=0,1,\ldots,N-1$.

Based on the assumed stationarity of $y(t)$ and a type of the central limit theorem, the real and imaginary part of the FFT at nonzero frequencies are Gaussian distributed with zero mean as $N\to\infty$ (Brillinger 1969; Yajima 1989; Yuen et al. 2002). Therefore, the estimator $S_{y,N}(\omega_k)$, $k=1,\ldots,N_1-1$, has the following asymptotic behavior:

$$\lim_{N\to\infty}S_{y,N}(\omega_k)=\frac{1}{2}S_y(\omega_k)\chi_2 \tag{9}$$

where χ_2 = a random variable having chi-square distribution with two degrees of freedom (i.e., exponential distribution) (Yaglom 1987). Therefore, the PDF of the random variable $Y(\omega_k)=\lim_{N\to\infty}S_{y,N}(\omega_k)$ is asymptotically given by

$$p(Y(\omega_k)|\mathbf{a})=\frac{1}{S_y(\omega_k)}\exp\left[-\frac{Y(\omega_k)}{S_y(\omega_k)}\right] \tag{10}$$

where $S_y(\omega_k)$ depends on the model parameter vector $\mathbf{a}$.

In the case of finite N, it can be shown using simulations that for $k\ll N_1$, the PDF of $S_{y,N}(\omega_k)$ can be accurately approximated by an exponential distribution in analogy to Eq. (10) except that the mean $S_y(\omega_k)$ is replaced by $E[S_{y,N}(\omega_k)]$ given by Eq. (7). Note that this approximation is very accurate regardless of the true probability distribution of $y(n\Delta t)$, $n=1,\ldots,N$ (Yajima 1989; Yuen et al. 2002). This is due to the robustness of the Gaussian approximation of the probability distribution of the FFT with respect to the probability distribution of the stationary response signal.

Furthermore, the random variables $S_{y,N}(\omega_k)$ and $S_{y,N}(\omega_\ell)$ with $k\neq\ell$ and k, $\ell\ll N_1$, are uncorrelated asymptotically as $N\to\infty$ (Yuen et al. 2002). Note that uncorrelated exponential random variables are independent (Yaglom 1987). For large N, this property is approximately correct in a certain frequency range. In particular, for a sufficiently small number $K<N_1$, one can assume that the random vector $\mathbf{S}_{y,N}^K=[S_{y,N}(\omega_1),\ldots,S_{y,N}(\omega_K)]^T$ has

all its elements approximately independently exponentially distributed. Therefore, its joint PDF can be approximated as follows:

$$p(\mathbf{S}_{y,N}^K|\mathbf{a}) \simeq \prod_{k=1}^{K} \frac{1}{E[S_{y,N}(\omega_k)]} \exp\left(-\frac{S_{y,N}(\omega_k)}{E[S_{y,N}(\omega_k)]}\right) \quad (11)$$

where $E[S_{y,N}(\omega_k)]$ is given by Eq. (7) and it depends on the model parameter vector $\mathbf{a}$. In practice, ω_K can be chosen in the range $[1.5\omega_\rho, 2.0\omega_\rho]$ where ω_ρ is the frequency at which the peak of the spectral estimates $\hat{\mathbf{S}}_{y,N}(\omega_k)$ occurs. A more detailed discussion will be given in the numerical examples.

Given the observed data $\hat{\mathbf{Y}}_N$, one may substitute it into Eq. (5) to calculate the corresponding observed spectral estimate $\hat{\mathbf{S}}_{y,N}^K = [\hat{S}_{y,N}(\omega_1),\ldots,\hat{S}_{y,N}(\omega_K)]^T$. Using Bayes' theorem, the updated PDF of the model parameters $\mathbf{a}$ given the data $\hat{\mathbf{S}}_{y,N}^K$ follows from an analogy to Eq. (4):

$$p(\mathbf{a}|\hat{\mathbf{S}}_{y,N}^K) = c_2 p(\mathbf{a}) p(\hat{\mathbf{S}}_{y,N}^K|\mathbf{a}). \quad (12)$$

where c_2 = a normalizing constant, and the likelihood $p(\hat{\mathbf{S}}_{y,N}^K|\mathbf{a})$ is given by Eq. (11) where each $S_{y,N}(\omega_k)$ is replaced by $\hat{S}_{y,N}(\omega_k)$, and $E[S_{y,N}(\omega_k|\mathbf{a})]$ is calculated from Eq. (7) where $R_x(n\Delta t) = R_x(n\Delta t|\mathbf{a})$ may be calculated by equivalent linearization methods or by simulation. The optimal parameters $\hat{\mathbf{a}}$ are obtained by minimizing the objective function $J(\mathbf{a}) = -\ln[p(\mathbf{a})p(\hat{\mathbf{S}}_{y,N}^K|\mathbf{a})]$. For the results in this paper, this optimization is done using a *MATLAB* function ''fmins'' (*MATLAB* 1994).

In the case where several independent time histories $\hat{\mathbf{Y}}_N^{(1)},\ldots,\hat{\mathbf{Y}}_N^{(M)}$ are available, the estimation can proceed by calculating the corresponding estimates $\hat{\mathbf{S}}_{y,N}^{K,(1)},\ldots,\hat{\mathbf{S}}_{y,N}^{K,(M)}$ and then calculating the updated PDF

$$p(\mathbf{a}|\hat{\mathbf{S}}_{y,N}^{K,(1)},\ldots,\hat{\mathbf{S}}_{y,N}^{K,(M)}) = c_3 p(\mathbf{a}) \prod_{n=1}^{M} p(\hat{\mathbf{S}}_{y,N}^{K,(n)}|\mathbf{a}) \quad (13)$$

where $p(\hat{\mathbf{S}}_{y,N}^{K,(n)}|\mathbf{a})$ is given by Eq. (11).

Note that in the proposed approach, each set of data can correspond to a different time duration T and different sampling time interval Δt and Eq. (13) automatically takes care of the weighting for different sets of data.

Multiple-Degree-of-Freedom Systems

Model Formulation

Consider a system with N_d degrees of freedom (DOFs) whose displacement response $\mathbf{x}(t) \in \mathbb{R}^{N_d}$ is modeled using the equation of motion:

$$\mathbf{M}\ddot{\mathbf{x}} + \mathbf{f}_s(\mathbf{x},\dot{\mathbf{x}};\boldsymbol{\theta}_s) = \mathbf{T}\mathbf{f}(t) \quad (14)$$

where $\mathbf{M} \in \mathbb{R}^{N_d \times N_d}$ = the (known) mass matrix, $\mathbf{f}_s \in \mathbb{R}^{N_d}$ = the nonlinear restoring force characterized by the structural parameters $\boldsymbol{\theta}_s$, $\mathbf{T} \in \mathbb{R}^{N_d \times N_f}$ = a force distribution matrix, and $\mathbf{f}(t) \in \mathbb{R}^{N_f}$ = an external excitation (e.g., force or ground acceleration) modeled by a stationary Gaussian process with zero mean and spectral density matrix function characterized by the excitation parameters θ_f:

$$\mathbf{S}_f(\omega) = \mathbf{S}_f(\omega;\boldsymbol{\theta}_f) \quad (15)$$

Assume now that discrete response data are available for $N_o (\leq N_d)$ observed DOFs. Let Δt denote the sampling time step. Because of measurement noise and modeling errors, the measured response $\mathbf{y}(n) \in \mathbb{R}^{N_o}$ (at time $t = n\Delta t$) will differ from the model response $\mathbf{q}(n)$, e. g., model displacement or model acceleration, calculated at the observed DOFs from Eq. (14). This difference between the measured and model response, called prediction error, is modeled as a discrete zero-mean Gaussian white noise vector process $\boldsymbol{\eta}(n) \in \mathbb{R}^{N_o}$ so

$$\mathbf{y}(n) = \mathbf{q}(n) + \boldsymbol{\eta}(n) \quad (16)$$

where the discrete process $\boldsymbol{\eta}$ is independent of $\mathbf{q}$ and satisfies

$$E[\boldsymbol{\eta}(n)\boldsymbol{\eta}^T(p)] = \boldsymbol{\Gamma}_\eta \delta_{np} \quad (17)$$

where $E[.]$ = expectation, δ_{np} = the Kronecker delta function, and $\boldsymbol{\Gamma}_\eta$ = the $N_o \times N_o$ covariance matrix of the prediction–error process $\boldsymbol{\eta}$.

Let $\mathbf{a}$ denote the parameter vector for identification; it includes the following parameters: (1) the structural parameters $\boldsymbol{\theta}_s$; (2) the excitation parameters $\boldsymbol{\theta}_f$; and (3) the elements of the upper right triangular part of $\boldsymbol{\Gamma}_\eta$ (symmetry defines the lower triangular part of this matrix). As in the SDOF case, we apply Bayes' theorem to update the uncertainty regarding the values of the model parameters $\mathbf{a}$ based on the spectral density estimates.

Spectral Density Estimator and its Statistical Properties

Consider the stationary stochastic vector process $\mathbf{y}(t)$ and a finite number of discrete data $\mathbf{Y}_N = \{\mathbf{y}(n), n = 0,\ldots,N-1\}$. Based on $\mathbf{Y}_N$, we introduce the following discrete estimator of the $N_o \times N_o$ spectral density matrix of the stochastic process $\mathbf{y}(t)$:

$$\mathbf{S}_{y,N}(\omega_k) = \boldsymbol{\mathcal{Y}}_N(\omega_k)\overline{\boldsymbol{\mathcal{Y}}}_N^T(\omega_k) \quad (18)$$

where $\overline{z}$ = the complex conjugate of a complex variable z and $\boldsymbol{\mathcal{Y}}_N(\omega_k)$ = the (scaled) discrete Fourier Transform of the vector process $\mathbf{y}$ at frequency ω_k, as follows:

$$\boldsymbol{\mathcal{Y}}_N(\omega_k) = \sqrt{\frac{\Delta t}{2\pi N}} \sum_{n=0}^{N-1} \mathbf{y}(n)\exp(-i\omega_k n\Delta t) \quad (19)$$

where $\omega_k = k\Delta\omega$, $k = 0,\ldots,N_1-1$ with $N_1 = \mathrm{INT}(N/2)$, $\Delta\omega = 2\pi/T$, and $T = N\Delta t$. Note that $\mathbf{S}_{y,N}(\omega_k)$ contains estimates of the autospectral densities in its diagonal elements and estimates of the cross-spectral densities in its off-diagonal elements. Note also that Eq. (5) is a special case of Eqs. (18) and (19).

Using Eqs. (16) and taking expectation of Eq. (18) (noting that $\mathbf{q}$ and $\boldsymbol{\eta}$ are independent) yields

$$E[\mathbf{S}_{y,N}(\omega_k)|\mathbf{a}] = E[\mathbf{S}_{q,N}(\omega_k)|\mathbf{a}] + E[\mathbf{S}_{\eta,N}(\omega_k)|\mathbf{a}] \quad (20)$$

where $\mathbf{S}_{q,N}(\omega_k)$ and $\mathbf{S}_{\eta,N}(\omega_k)$ are defined in a manner similar to that described by Eqs. (18) and (19). It easily follows from Eqs. (17) and (18) that

$$E[\mathbf{S}_{\eta,N}(\omega_k)|\mathbf{a}] = \frac{\Delta t}{2\pi}\boldsymbol{\Gamma}_\eta \equiv \mathbf{S}_{\eta 0} \quad (21)$$

The term $E[\mathbf{S}_{q,N}(\omega_k)|\mathbf{a}]$ in Eq. (20) can also be evaluated by noting that $\mathbf{S}_{q,N}(\omega_k)$ has elements:

$$S_{q,N}^{(j,\ell)}(\omega_k) = \frac{\Delta t}{2\pi N} \sum_{n,p=0}^{N-1} q_j(n) q_\ell(p) e^{-i\omega_k(n-p)\Delta t} \quad (22)$$

Grouping together terms having the same value of $(p-n)$ in Eq. (22), and taking expectation, we obtain the following expression:

$$E[S_{q,N}^{(j,\ell)}(\omega_k)|\mathbf{a}]=\frac{\Delta t}{4\pi N}\sum_{n=0}^{N-1}\gamma_n[R_q^{(j,\ell)}(n\Delta t|\mathbf{a})e^{-i\omega_k n\Delta t}$$

$$+R_q^{(j,\ell)}(-n\Delta t|\mathbf{a})e^{i\omega_k n\Delta t}] \tag{23}$$

where γ_n is given by Eq. (8) and $R_q^{(j,\ell)}$ = the cross-correlation functions between the jth and ℓth component of the model quantity $\mathbf{q}$. However, it is usually not possible to obtain the correlation functions theoretically. In this case, for given $\mathbf{a}$, we can simulate samples of the response using Eqs. (14) and (15) and hence calculate their spectral density estimates in a similar manner to that described in Eqs. (18) and (19). Then, rather than using Eq. (23), the expected values of the spectral estimates can be approximated by the average of the spectral density estimators obtained from the samples.

Next, we discuss the statistical properties of the estimator $\mathbf{S}_{y,N}(\omega_k)$. Denote by $\mathcal{Y}_{N,R}(\omega_k)$ and $\mathcal{Y}_{N,I}(\omega_k)$ the real and imaginary part, respectively, of $\mathcal{Y}_N(\omega_k)$, that is, $\mathcal{Y}_N(\omega_k)=\mathcal{Y}_{N,R}(\omega_k)+i\mathcal{Y}_{N,I}(\omega_k)$. Since $\mathcal{Y}(\boldsymbol{\omega}_\mathbf{k})_N$ is zero-mean and asymptotically a Gaussian vector for $k=1,\ldots,N_1-1$ (Brillinger 1969; Yajima 1989; Yuen et al. 2002), both $\mathcal{Y}_{N,R}(\omega_k)$ and $\mathcal{Y}_{N,I}(\omega_k)$ are also zero-mean Gaussian vectors as $N\to\infty$. Furthermore, in the limit when $N\to\infty$, the covariance matrix of the vector $[\mathcal{Y}_{N,R}^T(\omega_k),\mathcal{Y}_{N,I}^T(\omega_k)]^T$ has the form (Yuen 1999):

$$\mathbf{C}_N(\omega_k)=\begin{bmatrix}\mathbf{C}_{N,1}(\omega_k) & \mathbf{C}_{N,2}(\omega_k)\\ -\mathbf{C}_{N,2}(\omega_k) & \mathbf{C}_{N,1}(\omega_k)\end{bmatrix} \tag{24}$$

Eq. (24) states that the real and imaginary part of $\mathcal{Y}_N(\omega_k)$ have equal covariance matrices $\mathbf{C}_{N,1}(\omega_k)$ for $k=1,\ldots,N_1-1$, i.e., excluding the zero and Nyquist frequencies. Also, it states that the cross covariance between the real and imaginary part has the property $\mathbf{C}_{N,2}^T(\omega_k)=-\mathbf{C}_{N,2}(\omega_k)$, i.e., $E[\mathcal{Y}_{N,R}^{(j)}(\omega_k)\mathcal{Y}_{N,I}^{(\ell)}(\omega_k)]=-E[\mathcal{Y}_{N,R}^{(\ell)}(\omega_k)\mathcal{Y}_{N,I}^{(j)}(\omega_k)]$. The latter property implies also that the diagonal elements of $\mathbf{C}_{N,2}$ are equal to zero, i.e., $E[\mathcal{Y}_{N,R}^{(j)}(\omega_k)\mathcal{Y}_{N,I}^{(j)}(\omega_k)]=0$, for every j and ω_k. Because of Eq. (24), the complex vector $\mathcal{Y}_N(\omega_k)$ is said to have a complex multivariate normal distribution (Krishnaiah 1976) as $N\to\infty$.

Assume now that there is a set of independent, identically distributed, time histories $\mathbf{Y}_N^{(1)},\ldots,\mathbf{Y}_N^{(M)}$. As $N\to\infty$, the corresponding Fourier transforms $\mathcal{Y}_N^{(n)}(\omega_k)$, $n=1,\ldots,M$, are independent and follow an identical complex N_o-variate normal distribution with zero mean for $k=1,\ldots,N_1-1$. Then, if $M\geq N_o$, the average spectral density estimate (an $N_o\times N_o$ Hermitian matrix):

$$\mathbf{S}_{j,N}^M(\omega_k)=\frac{1}{M}\sum_{n=1}^{M}\mathbf{S}_{y,N}^{(n)}(\omega_k)=\frac{1}{M}\sum_{n=1}^{M}\mathcal{Y}_N^{(n)}(\omega_k)\bar{\mathcal{Y}}_N^{(n)T}(\omega_k) \tag{25}$$

follows a central complex Wishart distribution of dimension N_o with M DOF and mean $E[\mathbf{S}_{y,N}^M(\omega_k)]=E[\mathbf{S}_{y,N}(\omega_k)]=2[\mathbf{C}_{N,1}(\omega_k)-i\mathbf{C}_{N,2}(\omega_k)]$ as $N\to\infty$ (Krishnaiah 1976). The PDF of this distribution is given by

$$p(\mathbf{S}_{y,N}^M(\omega_k))=c_4\frac{|\mathbf{S}_{y,N}^M(\omega_k)|^{M-N_o}}{|E[\mathbf{S}_{y,N}(\omega_k)]|^M}$$

$$\times\exp(-Mtr\{E[\mathbf{S}_{y,N}(\omega_k)]^{-1}\mathbf{S}_{y,N}^M(\omega_k)\}) \tag{26}$$

where c_4 = a normalizing constant and $|\mathbf{A}|$ and $tr[\mathbf{A}]$ are the determinant and the trace, respectively, of a matrix $\mathbf{A}$. Note that this approximation is very accurate even if $y(n\Delta t)$, $n=0,\ldots,N-1$, is not Gaussian. Again, this is due to the robustness of the Gaussian approximation of the FFT irrespective of the probability distribution of the stationary response signal.

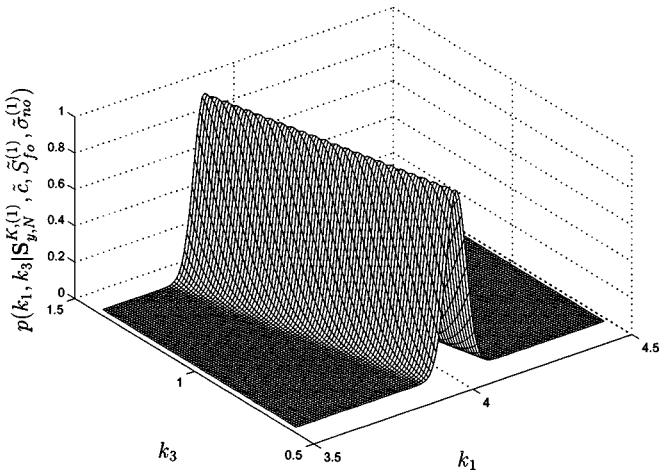

Fig. 1. Conditional updated probability density function $p(k_1,k_3|\hat{\mathbf{S}}_{y,N}^{K,(1)},\tilde{c},\tilde{S}_{fo}^{(1)},\tilde{\sigma}_{\eta o}^{(1)})$ (Example 1)

Also, note that in the special case of a SDOF oscillator or in the case of a MDOF system with only one set of data at one measured DOF ($M=1$ and $N_o=1$), the distribution in Eq. (26) becomes an exponential distribution and so reduces to Eq. (10).

Furthermore, when $N\to\infty$, the vectors $[\mathcal{Y}_{N,R}^T(\omega_k),\mathcal{Y}_{N,I}^T(\omega_k)]^T$ and $[\mathcal{Y}_{N,R}^T(\omega_\ell),\mathcal{Y}_{N,I}^T(\omega_\ell)]^T$ with $\omega_k\neq\omega_\ell$ are independent (Yuen et al. 2002). This causes the complex vectors $\mathcal{Y}_N(\omega_k)$ and $\mathcal{Y}_N(\omega_\ell)$ to be independent (as $N\to\infty$). As a result, the matrices $\mathbf{S}_{y,N}^M(\omega_k)$ and $\mathbf{S}_{y,N}^M(\omega_\ell)$ are independently Wishart distributed for $k\neq\ell$, that is,

$$p[\mathbf{S}_{y,N}^M(\omega_k),\mathbf{S}_{y,N}^M(\omega_\ell)]=p[\mathbf{S}_{y,N}^M(\omega_k)]p[\mathbf{S}_{y,N}^M(\omega_\ell)] \tag{27}$$

where the two right-hand side factors are given by Eq. (26). Although Eqs. (26) and (27) are correct only asymptotically as $N\to\infty$, it was shown by simulations that these are indeed very accurate approximations in a certain bandwidth of frequencies for the case where N is finite (Yuen 1999). In the case of displace-

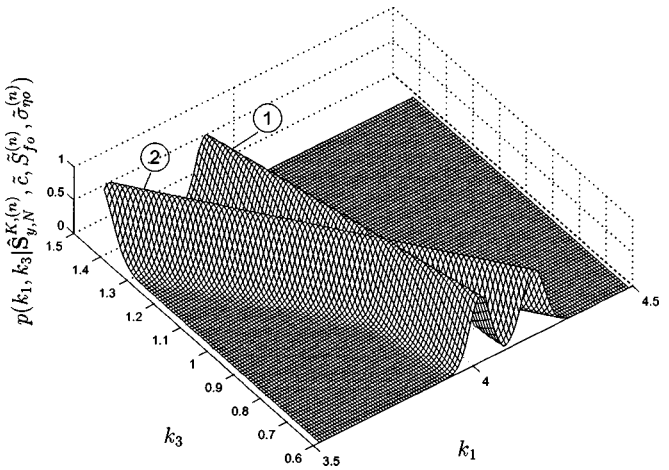

Fig. 2. Conditional updated probability density function $p(k_1,k_3|\hat{\mathbf{S}}_{y,N}^{K,(n)},\tilde{c},\tilde{S}_{fo}^{(n)},\tilde{\sigma}_{\eta o}^{(n)})$, $n=1,2$ (Example 1)

Table 1. Comparison of Actual Parameters Versus Optimal Estimates and Their Statistics for Duffing Oscillator (Example 1)

Parameter	Actual $\tilde{a}$	Optimal $\hat{a}$	Standard deviation σ	COV $\alpha=\frac{\sigma}{\tilde{a}}$	$\beta=\frac{\lvert\tilde{a}-\hat{a}\rvert}{\sigma}$
c	0.1000	0.1021	0.0108	0.108	0.20
k_1	4.0000	3.9420	0.0463	0.012	1.25
k_3	1.0000	0.9868	0.1295	0.130	0.10
$S_{fo}^{(1)}$	0.0100	0.0098	0.0005	0.046	0.41
$S_{fo}^{(2)}$	0.0400	0.0454	0.0020	0.051	2.64
$\sigma_{\eta o}^{(1)}$	0.0526	0.0514	0.0022	0.042	0.55
$\sigma_{\eta o}^{(2)}$	0.1092	0.1025	0.0045	0.041	1.49

ments (or accelerations), such range of frequencies corresponds to the lower- (or higher-) frequency range $\omega_k \in [\omega_1, \omega_K]$ (or $[\omega_K, \omega_{N_1-1}]$).

Identification Based on Spectral Density Estimates

Based on the aforementioned discussion regarding the statistical properties of the average spectral estimator $\mathbf{S}_{y,N}^{M}(\omega_k)$, a Bayesian approach for updating the PDF of the uncertain parameter vector $\mathbf{a}$ is proposed as follows: Given $M \geq N_0$ (where N_0 = the number of observed DOF) independent sets of observed data $\hat{\mathbf{Y}}_N^{(n)}$, $n=1,\ldots,M$, one may calculate the corresponding observed spectral estimate matrices $\hat{\mathbf{S}}_{y,N}^{(n)}$, $n=1,\ldots,M$ using Eqs. (18) and (19). Next, one can calculate the average matrix estimates $\hat{\mathbf{S}}_{y,N}^{(M)}(\omega_k)$ using Eq. (25) and then form the set $\hat{\mathbf{S}}_{y,N}^{M,K} = \{\hat{\mathbf{S}}_{y,N}^{M}(k\Delta\omega),\ k=1,\ldots,K\}$, where K is an integer sufficiently smaller than $N_1 = \mathrm{INT}(N/2)$. Using Bayes' theorem, the updated PDF of the model parameters $\mathbf{a}$, given the data $\hat{\mathbf{S}}_{y,N}^{M,K}$, is then given by

$$p(\mathbf{a}|\hat{\mathbf{S}}_{y,N}^{M,K}) = c_5 p(\mathbf{a}) p(\hat{\mathbf{S}}_{y,N}^{M,K}|\mathbf{a}) \tag{28}$$

where c_5 = a normalizing constant such that the integral of the right-hand side of Eq. (28) over the domain of $\mathbf{a}$ is equal to one. The factor $p(\mathbf{a})$ in the Eq. (28) represents the prior PDF, which expresses the relative plausibilities of different values of a based on prior information and engineering judgment. The likelihood factor $p(\hat{\mathbf{S}}_{y,N}^{M,K}|\mathbf{a})$ expresses the contribution of the observed data. Based on Eqs. (26) and (27), this factor can be calculated as follows:

$$p(\hat{\mathbf{S}}_{y,N}^{M,K}|\mathbf{a}) \simeq c_6 \prod_{k=1}^{K} \frac{|\hat{\mathbf{S}}_{y,N}^{M}(\omega_k)|^{M-N_0}}{|E[\mathbf{S}_{y,N}(\omega_k)|\mathbf{a}]|^{M}} \times \exp(-M\ tr\{E[\mathbf{S}_{y,N}(\omega_k)|\mathbf{a}]^{-1}\hat{\mathbf{S}}_{y,N}^{M}(\omega_k)\}) \tag{29}$$

where $E[\mathbf{S}_{y,N}(\omega_k)|\mathbf{a}]$ is given by Eqs. (20) and (21) with $E[\mathbf{S}_{q,N}(\omega_k)|\mathbf{a}]$ estimated by simulation as explained earlier. It is suggested to choose ω_K such that the frequency range just includes all of the peaks of the spectral density estimates. A more detailed discussion will be given in the third example.

The most probable parameters $\hat{\mathbf{a}}$ are obtained by minimizing the objective function $J(\mathbf{a}) = -\ln[p(\mathbf{a})p(\hat{\mathbf{S}}_{y,N}^{M,K}|\mathbf{a})]$. Furthermore, for large amounts of data (large product KN_0M), the updated PDF $p(\mathbf{a}|\hat{\mathbf{S}}_{y,N}^{M,K})$ can be approximated by a Gaussian distribution centered at the optimal point $\hat{\mathbf{a}}$ if it is globally identifiable (Beck and Katafygiotis 1998). The corresponding covariance matrix $\mathbf{\Gamma}_a$ is equal to the inverse of the Hessian matrix of the function $J(\mathbf{a}) = -\ln[p(\mathbf{a}|\hat{\mathbf{S}}_{y,N}^{M,K})]$ calculated at $\mathbf{a}=\hat{\mathbf{a}}$, i.e., $\mathbf{\Gamma}_a = \mathbf{H}(\hat{\mathbf{a}})^{-1}$ where $H_{j\ell}(\hat{\mathbf{a}}) = \partial^2 J(\mathbf{a})/\partial a_j \partial a_\ell|_{\mathbf{a}=\hat{\mathbf{a}}}$. In the results presented in

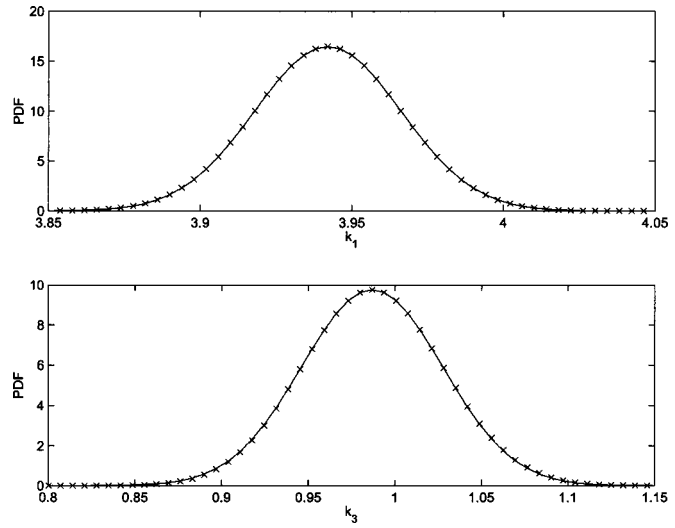

Fig. 3. Conditional probability density function of k_1 and k_3 calculated using: (1) Eq. (13)—crosses; and (2) Gaussian approximation—solid. The remaining parameters are fixed at their optimal values.

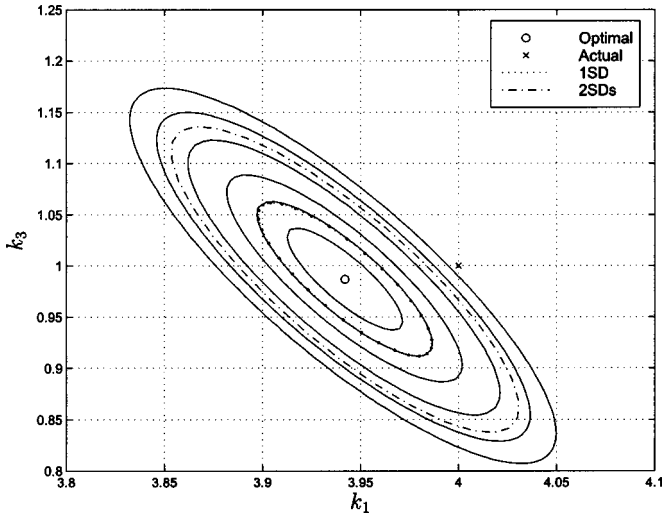

Fig. 4. Contours in the (k_1, k_3) plane of conditional updated probability density function $p(k_1, k_3|\hat{\mathbf{S}}_{y,N}^{K,(1)}, \hat{\mathbf{S}}_{y,N}^{K,(2)}, \hat{c}, \hat{S}_{fo}^{(1)}, \hat{S}_{fo}^{(2)}, \hat{\sigma}_{\eta o}^{(1)}, \hat{\sigma}_{\eta o}^{(2)})$ (Example 1).

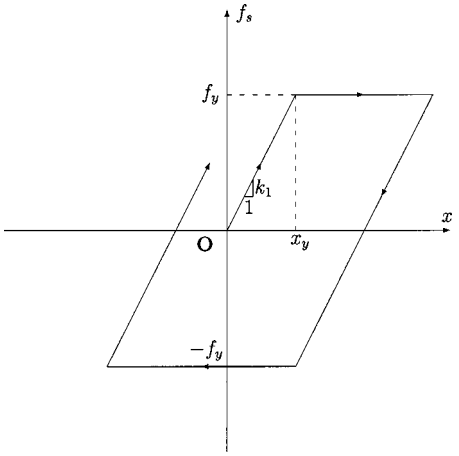

Fig. 5. Relationship between restoring force and displacement of system (Example 2).

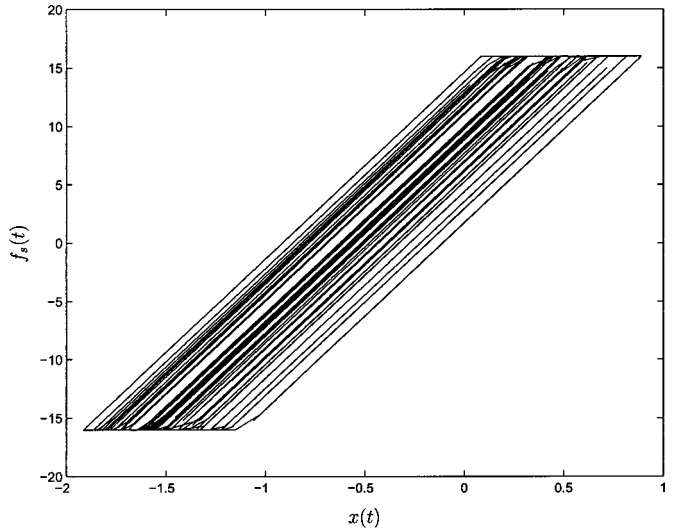

Fig. 6. Hysteresis loops of simulated data (Example 2)

this paper, this Hessian matrix is calculated using a finite difference method. This Gaussian approximation provides a very efficient way for the quantification of the uncertainty for the model parameters without evaluating high-dimensional integrals. However, it is not always a very accurate approximation, e.g., in unidentifiable cases. One check is to assume that the Gaussian approximation is accurate and calculate some lower-dimensional conditional PDFs and compare them with the values calculated from Eq. (28). If they match well, then the approximation can be used. If they do not match, simulation methods may be used (e.g., Beck and Au 2002) to calculate the associated uncertainties for the parameters.

Numerical Examples

Example 1: Duffing Oscillator

In this example, we consider a SDOF Duffing oscillator of known mass m subjected to zero-mean stationary Gaussian white noise $f(t)$ with spectral intensity S_{fo}:

$$m\ddot{x}(t)+c\dot{x}(t)+k_1x(t)+k_3x^3(t)=f(t) \tag{30}$$

To simulate noisy data, the stationary displacement response history $\hat{\mathbf{Y}}_N^{(1)}$ was generated with parameters $\tilde{\mathbf{a}}=[\tilde{c},\tilde{k}_1,\tilde{k}_3,\tilde{S}_{fo}^{(1)},\tilde{\sigma}_{\eta o}^{(1)}]^T$ where $m=1$ kg, $\tilde{c}=0.1$ kg/s, $\tilde{k}_1=4.0$ N/m, $\tilde{k}_3=1.0$ N/m^3, $\tilde{S}_{fo}^{(1)}=0.01$ N^2 s and $\tilde{\sigma}_{\eta o}^{(1)}=0.0526$ m (20% noise). The sampling interval is $\Delta t=0.1$ s, with total time $T=1{,}000$ s, so $N=10{,}000$.

Multiplying Eq. (30) with $x(t-\tau)$ and taking expectation yields

$$mR_x''(\tau)+cR_x'(\tau)+k_1R_x(\tau)+k_3E[x(t-\tau)x^3(t)]=0 \tag{31}$$

where $R_x(\tau)\equiv E[x(t-\tau)x(t)]$, $\forall t\in\mathbb{R}$. The term $E[x(t-\tau)x^3(t)]$ can be approximated by neglecting the fourth cumulant term, that is, $E[x(t-\tau)x^3(t)]\approx 3\sigma_x^2R_x(\tau)$, where $\sigma_x^2=R_x(0)$ is the variance of the response (Lutes and Sarkani 1997). Therefore, a differential equation for an approximation of the response autocorrelation function can be readily obtained:

$$mR_x''(\tau)+cR_x'(\tau)+(k_1+3\sigma_x^2k_3)R_x(\tau)=0 \tag{32}$$

with $R_x(0)=\sigma_x^2$ and $R_x'(0)=0$. Eq. (32) is a second-order ordinary differential equation with constant coefficients, which can be solved analytically. Then, $E[S_{y,N}(\omega_k)|\mathbf{a}]$ can be obtained for a given parameter vector $\mathbf{a}$ by using Eq. (7). Finally, the updated PDF $p(\mathbf{a}|\hat{\mathbf{S}}_{y,N}^{K,(1)})$ is readily obtained using Eqs. (5), (11), and (12), where we take $p(\mathbf{a})$ as constant over the region where $p(\hat{\mathbf{S}}_{y,N}^{K,(1)}|\mathbf{a})$ is large, i.e., a locally noninformative prior PDF (Box and Tiao 1973).

Fig. 1 shows the conditional posterior PDF $p(k_1,k_3|\hat{\mathbf{S}}_{y,N}^{K,(1)},\tilde{c},\tilde{S}_{fo}^{(1)},\tilde{\sigma}_{\eta o}^{(1)})$ normalized in such a way that the peak value is unity, which is obtained by utilizing only the spectral estimates up to frequency $\omega_K=1.0$ Hz ($K=1{,}000$). Note that the small-amplitude natural frequency of the oscillator is $1/\pi$ Hz≈ 0.32 Hz. It is obvious that this case is unidentifiable, i.e., given one set of dynamic data, the estimates of k_1 and k_3 suffer from large uncertainty as there are infinitely many combinations of k_1 and k_3 which give similar values for the posterior PDF.

Another time history data set $\hat{\mathbf{Y}}_N^{(2)}$ was generated for the same oscillator (same $\tilde{c}$, $\tilde{k}_1$, and $\tilde{k}_3$) but with $\tilde{S}_{fo}^{(2)}=0.04$ N^2 s and $\tilde{\sigma}_{\eta o}^{(2)}=0.1092$ m (20% noise). This case is, again, unidentifiable.

Table 2. Identification Results for Elastoplastic System with Theoretical Spectrum Estimated by Equivalent Linearization (Example 2)

Parameter	Actual $\tilde{a}$	Optimal $\hat{a}$	Standard deviation σ	COV $\alpha=\dfrac{\sigma}{\tilde{a}}$	$\beta=\dfrac{\lvert\tilde{a}-\hat{a}\rvert}{\sigma}$
k_1	16.000	15.827	0.1162	0.007	1.49
x_y	1.0000	1.3493	0.4818	0.482	0.72
σ_x	0.6029	0.5762	0.1437	0.238	0.19
$\sigma_{\eta o}$	0.1206	0.1376	0.0209	0.173	0.82

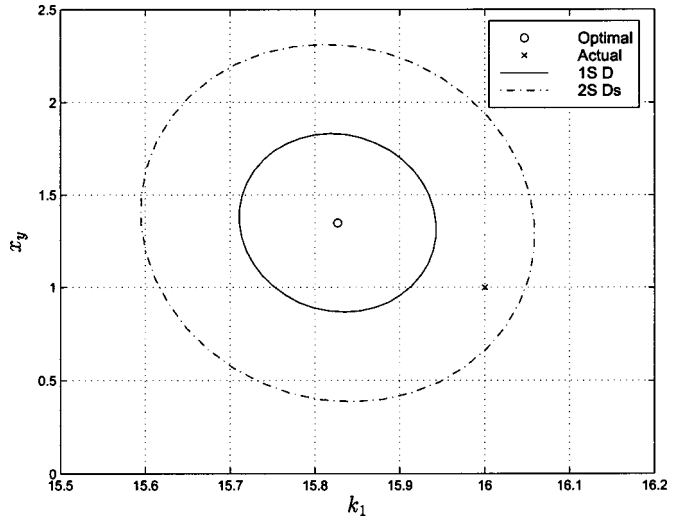

Fig. 7. Contours of conditional updated probability density function $p(k_1, x_y | \hat{\mathbf{S}}_{y,N}^K, \hat{\sigma}_x, \hat{\sigma}_{\eta o})$ with the theoretical spectrum estimated by equivalent linearization (Example 2)

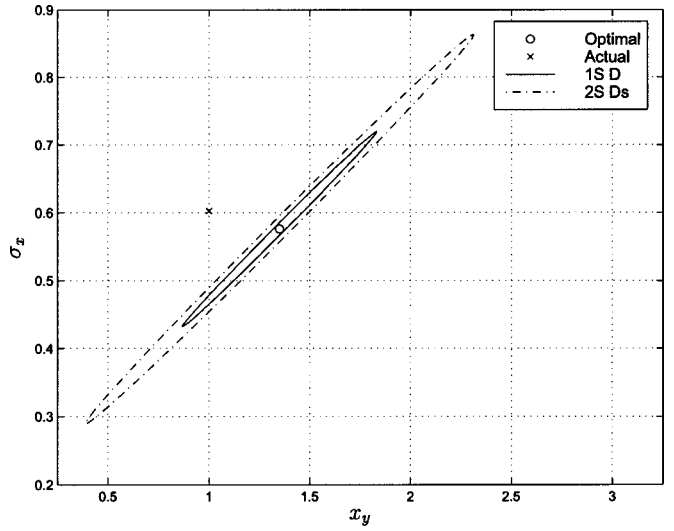

Fig. 9. Contours of conditional updated probability density function $p(x_y, \sigma_x | \hat{\mathbf{S}}_{y,N}^K, \hat{k}_1, \hat{\sigma}_{\eta o})$ with the theoretical spectrum estimated by equivalent linearization (Example 2)

However, if we plot these two posterior PDFs together (shown in Fig. 2), the peak trajectories in the (k_1, k_3) plane have different slopes. By Eq. (32), the equivalent linear system has a stiffness $k_1 + 3\sigma_x^2 k_3$. Therefore, the autocorrelation coefficients depend on σ_x and, hence, the level of excitation S_{f0}, showing that different levels of excitation lead to different slopes of the peak trajectories in the (k_1, k_3) plane. Since the coefficient $3\sigma_x^2$ is always positive, the slope of the peak trajectories in the (k_1, k_3) plane is always negative. This is expected because a larger value of k_1 can compensate for a smaller value of k_3, and vice versa.

Fig. 2 suggests that if we use the two dynamic data sets $\hat{\mathbf{Y}}_N^{(1)}$ and $\hat{\mathbf{Y}}_N^{(2)}$ together, uncertainty in k_1 and k_3 can be significantly reduced. Table 1 shows the estimated optimal values $\hat{\mathbf{a}} = [\hat{c}, \hat{k}_1, \hat{k}_3, \hat{S}_{fo}^{(1)}, \hat{S}_{fo}^{(2)}, \hat{\sigma}_{\eta o}^{(1)}, \hat{\sigma}_{\eta o}^{(2)}]^T$ and the calculated standard deviations σ_c, σ_{k_1}, σ_{k_3}, $\sigma_{S_{fo}^{(1)}}$, $\sigma_{S_{fo}^{(2)}}$, $\sigma_{\sigma_{\eta o}^{(1)}}$, and $\sigma_{\sigma_{\eta o}^{(2)}}$ obtained using both data sets $\hat{\mathbf{Y}}_N^{(1)}$ and $\hat{\mathbf{Y}}_N^{(2)}$. It also gives the coefficient of variation (COV) for the parameter estimates and a ''normalized error'' β. This normalized error parameter represents the absolute value of the difference between the identified optimal value and exact value, normalized with respect to the corresponding calculated standard deviation. The COVs in Table 1 are all quite small, showing that the parameter values are pinned down rather precisely by the data. The normalized errors β in Table 1 are of the order of 2 or less, suggesting that the procedure is not producing ''biased'' estimates, that is, the errors are not unusually large, compared to the calculated standard deviations.

Fig. 3 shows the conditional updated PDFs $p(k_1 | \hat{\mathbf{S}}_{y,N}^{K,(1)}, \hat{\mathbf{S}}_{y,N}^{K,(2)}, \hat{c}, \hat{k}_3, \hat{S}_{fo}^{(1)}, \hat{S}_{fo}^{(2)}, \hat{\sigma}_{\eta o}^{(1)}, \hat{\sigma}_{\eta o}^{(2)})$ and $p(k_3 | \hat{\mathbf{S}}_{y,N}^{K,(1)}, \hat{\mathbf{S}}_{y,N}^{K,(2)}, \hat{c}, \hat{k}_1, \hat{S}_{fo}^{(1)}, \hat{S}_{fo}^{(2)}, \hat{\sigma}_{\eta o}^{(1)}, \hat{\sigma}_{\eta o}^{(2)})$, obtained from: (1) Eq. (13) (crosses) and (2) the Gaussian approximation (solid line). It can be seen that the asymptotic Gaussian approximation is very accurate because 2,000 data points are involved in the likelihood function given by Eq. (13). This property provides a very efficient way for the quantification of the uncertainty for the model parameters, especially since the evaluation of high-dimensional integrals is not straightforward.

Fig. 4 shows nearly elliptical contours (solid lines) in the (k_1, k_3) plane of the conditional updated PDF $p(k_1, k_3 | \hat{\mathbf{S}}_{y,N}^{K,(1)}, \hat{\mathbf{S}}_{y,N}^{K,(2)}, \hat{c}, \hat{S}_{fo}^{(1)}, \hat{S}_{fo}^{(2)}, \hat{\sigma}_{\eta o}^{(1)}, \hat{\sigma}_{\eta o}^{(2)})$ calculated using Eq. (13) (keeping all the other parameters fixed at their optimal values). These contours correspond to the parameter sets, which give 80, 60, 40, 20, 10, and 5% of the conditional PDF values at its peak. Furthermore, by using the Gaussian approximation, the one- and two standard deviations contours can be calculated, which are shown by a dotted line and a dashed line, respectively, in Fig. 4. One can see that the orientation of the ellipses is the same for the two groups of contours, showing that the Gaussian approximation is very accurate in this case. Note that the optimal parameter values for k_1 and k_3 seem to be more than two standard deviations away from their actual values because Fig. 4 shows the conditional PDF, not the marginal PDF. Table 1 shows that the optimal estimates and actual values of k_1 and k_3 are much closer than two standard deviations.

The estimation of the model parameters $\boldsymbol{\theta}_s$ is not sensitive to the choice of the cutoff frequency ω_K as long as it is larger than the frequency at which the peak of the response spectral density

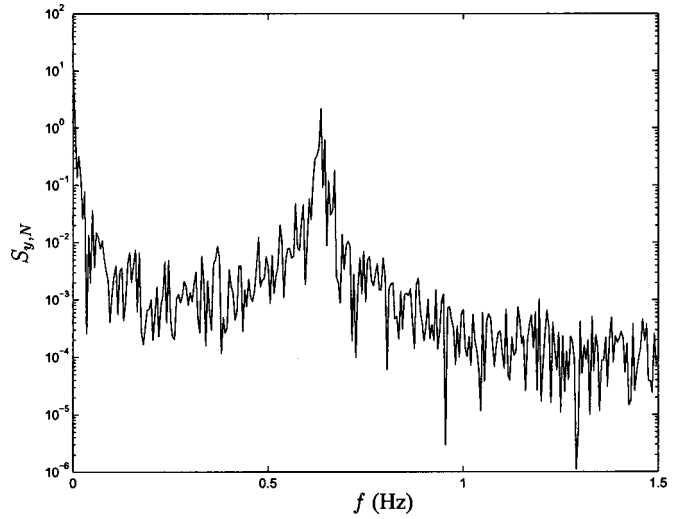

Fig. 8. Power spectral estimates using measurements (Example 2)

Table 3. Identification Results for Elastoplastic System with Theoretical Spectrum Estimated by Simulation (Example 2)

Parameter	Actual $\tilde{a}$	Optimal $\hat{a}$	Standard deviation σ	COV $\alpha=\frac{\sigma}{\tilde{a}}$	$\beta=\frac{\lvert\tilde{a}-\hat{a}\rvert}{\sigma}$
k_1	16.000	15.984	0.0433	0.003	0.36
x_y	1.0000	1.0918	0.0732	0.073	1.25
S_{fo}	0.1500	0.1376	0.0136	0.091	0.91
$\sigma_{\eta o}$	0.1206	0.1359	0.0201	0.166	0.76

estimates occurs. Identification using the same sets of data was also carried out with $\omega_K=5.0$ Hz (the Nyquist frequency, in this case). The results were virtually the same as those using $\omega_K=1.0$ Hz except that there were significant reductions in the uncertainty of the noise levels. That is, utilizing a larger ω_K gives better estimates for the noise level only. Therefore, it is suggested that one chooses an ω_K ranging from 1.5 ω_ρ to 2 ω_ρ where ω_ρ is the frequency at which the peak of the spectral estimates $\hat{\mathbf{S}}_{y,N}(\omega_k)$ occurs. It is computationally efficient to use such values of ω_K without sacrificing the quality of the identification for the model parameters $\boldsymbol{\theta}_s$.

Example 2: Elastoplastic Oscillator

In this example, we consider an elastoplastic SDOF oscillator of known mass m subjected to zero-mean stationary Gaussian white noise $f(t)$ with spectral intensity S_{fo}:

$$m\ddot{x}(t)+f_s(x(t))=f(t) \tag{33}$$

where $f_s(x(t))=$the restoring force of the system. The restoring force–displacement relationship is shown in Fig. 5. To simulate noisy data, the displacement response history $\hat{\mathbf{Y}}_N$ was generated with parameters $\tilde{\mathbf{a}}_0=[\tilde{k}_1,\tilde{x}_y,\tilde{S}_{fo},\tilde{\sigma}_{\eta o}]^T$ where $m=1$ kg, $\tilde{k}_1=16.0$ N/m, $\tilde{x}_y=1.0$ m, $\tilde{S}_{fo}=0.15$ N^2 s and $\tilde{\sigma}_{\eta o}=0.1206$ m (20% noise). The sampling rate interval is $\Delta t=0.05$ s, with a total time $T=200$ s, that is, $N=4{,}000$. The hysteresis loops of the simulated data are shown in Fig. 6. Note that these hysteresis loops are not assumed to be measured; they are shown here only for illustrative purposes. Note also that in this case, the displacement response is not perfectly stationary (Lutes and Sarkani 1997), but we show that the proposed identification method still produces satisfactory results.

The equivalent linear system has the following equation of motion:

$$m\ddot{x}(t)+b_2\dot{x}(t)+b_1x(t)=f(t) \tag{34}$$

where b_1 and b_2 are given by (Iwan and Lutes 1968; Lutes and Sarkani 1997):

$$b_1=k_1\left\{1-\frac{8}{\pi}\int_1^\infty\left[\frac{1}{z^3}+\frac{x_y^2}{2\sigma_x^2z}\sqrt{z-1}\exp\left(-\frac{x_y^2z^2}{2\sigma_x^2}\right)\right]dz\right\}$$

$$b_2=\sqrt{\frac{m}{2\pi b_1}}\frac{k_1x_y}{\sigma_x}\left[1-\mathrm{erf}\left(\frac{x_y}{\sqrt{2}\sigma_x}\right)\right] \tag{35}$$

Note that the calculation of b_1 and b_2 requires σ_x^2, the variance of the response. Although σ_x can be determined from the spectral intensity of the excitation S_{fo}, it is computationally more efficient to include σ_x directly instead of S_{fo} in the parameter vector. Therefore, the parameter vector $\mathbf{a}=[k_1,x_y,\sigma_x,\sigma_{\eta o}]^T$ is identified instead of $\mathbf{a}_o$ in this case. Then, $E[S_{y,N}(\omega_k)|\mathbf{a}]$ can be obtained given parameter vector $\mathbf{a}$ by using Eq. (7) where $R_x(n\Delta t)$ is approximated by the autocorrelation function for the equivalent linear system given by Eqs. (34) and (35). Finally, the updated PDF $p(\mathbf{a}|\hat{\mathbf{S}}_{y,N}^K)$ is readily obtained using Eqs. (5), (11), and (12). Note that a locally noninformative prior distribution is used, as in Example 1.

Table 2 shows the estimated optimal values $\hat{\mathbf{a}}=[\hat{k}_1,\hat{x}_y,\hat{\sigma}_x,\hat{\sigma}_{\eta o}]^T$ and the calculated standard deviations σ_{k_1},

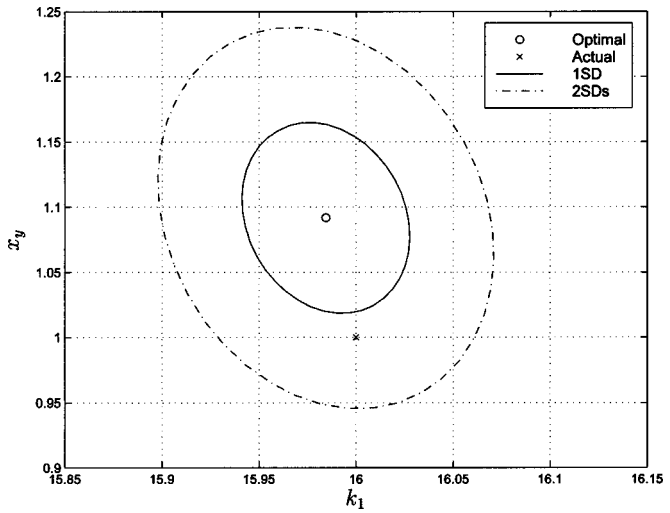

Fig. 10. Contours of conditional updated probability density function $p(k_1,x_y|\hat{\mathbf{S}}_{y,N}^K,\hat{\sigma}_x,\hat{\sigma}_{\eta o})$ with theoretical spectrum estimated by simulation (Example 2)

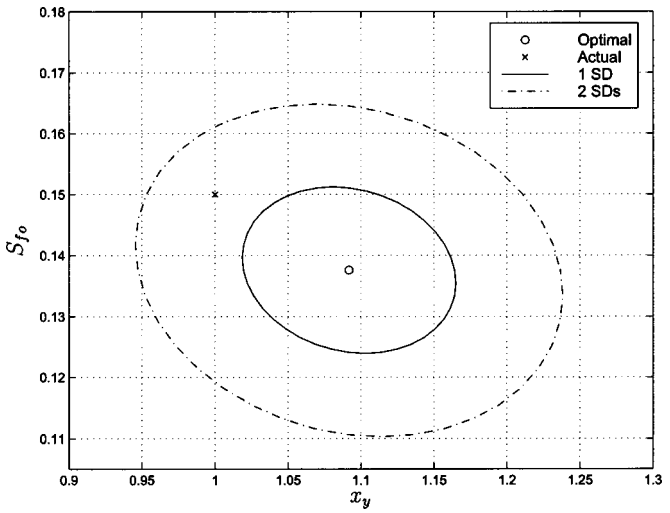

Fig. 11. Contours of conditional updated probability density function $p(x_y,S_{fo}|\hat{\mathbf{S}}_{y,N}^K,\hat{k}_1,\hat{\sigma}_{\eta o})$ with theoretical spectrum estimated using simulation (Example 2)

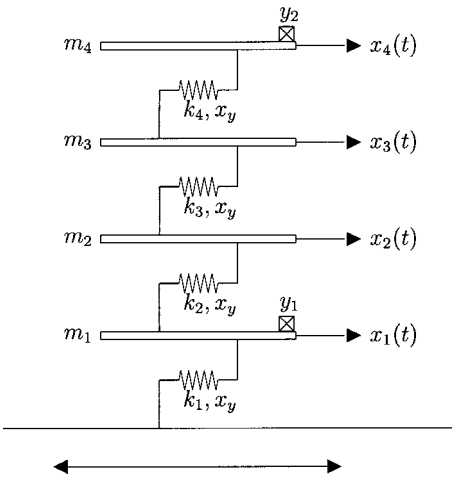

Fig. 12. Four-story inelastic structure (Example 3)

σ_{x_y}, σ_{σ_x}, and $\sigma_{\sigma_{\eta o}}$ obtained using the single data set $\hat{\mathbf{Y}}_N$. Fig. 7 shows contours in the (k_1, x_y) plane of the conditional updated PDF $p(k_1, x_y|\hat{\mathbf{S}}^K_{y,N}, \hat{\sigma}_x, \hat{\sigma}_{\eta o})$ calculated for one set of simulated data from Eq. (13) (keeping all the other parameters fixed at their optimal values). For these results, only the spectral estimates up to frequency $\omega_K = 1.25$ Hz ($K = 250$) were used. Note that the small-amplitude frequency of the oscillator is $2/\pi$ Hz$\approx$0.63 Hz. Again, ω_K can be chosen between 1.5 ω_ρ and 2.0 ω_ρ, as in Example 1, where from Fig. 8, the spectral estimates peak at $\omega_\rho \approx 0.65$ Hz.

Fig. 9 shows a similar plot to Fig. 7 but in the (x_y, σ_x) plane. It can be seen that the contours are very thin lying on the line $\sigma_x = \alpha_1 x_y + \alpha_2$, where $\alpha_1 \approx 0.28$ and $\alpha_2 \approx 0.2$, showing that the estimates of these parameters are very correlated. This is because b_1 and b_2 in Eq. (34) depend on m, k_1, and x_y/σ_x only. The only factor that makes x_y and σ_x identifiable comes from the amplitude of the spectrum, which is proportional to σ_x^2. This also explains why the uncertainty for x_y and σ_x is so large when utilizing equivalent linearization. Note from Table 2 that the actual values of the parameters $\tilde{x}_y$ and $\tilde{\sigma}_x$ are within one standard deviation from their optimal values $\hat{x}_y$ and $\hat{\sigma}_x$, respectively, but the actual

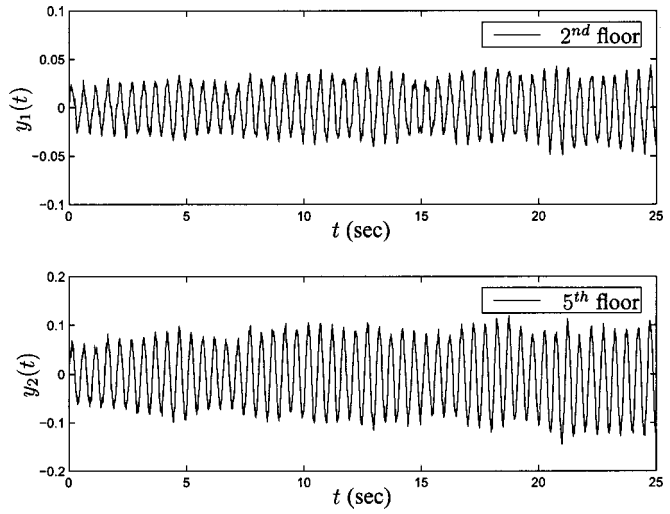

Fig. 13. Displacement measurements at second and fifth floor (Example 3)

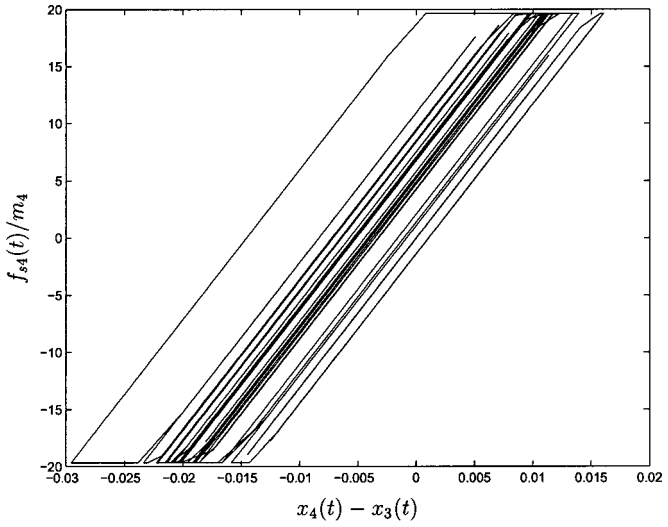

Fig. 14. Hysteresis loops for fourth story (Example 3)

parameters in the (x_y, σ_x) plane lie far outside the two standard deviations contour in Fig. 9. This is because Fig. 9 shows the conditional PDF, not the marginal PDF.

Table 3 shows the identification results using the same set of data with the theoretical spectrum estimated by simulation, rather than by using Eqs. (34) and (35). Note that in this case, the uncertain parameter vector is $\mathbf{a}_o = [k_1, x_y, S_{fo}, \sigma_{\eta o}]^T$, i.e., it includes the spectral intensity of the excitation instead of the root-mean-square (rms) of the response, because this is more efficient for the simulation of the system response. Here, for given parameter values, 100 samples of spectral estimates are simulated using Equations (33), (2), and (5) and the theoretical spectrum is approximated by the average of them. One can see that it gives more precise optimal parameter values than those in Table 2, especially for x_y, by comparing the respective COVs. This is because the equivalent linear system can not completely capture the dynamics of the nonlinear oscillator. Therefore, the results obtained by using an equivalent linear system lose some information from the data, suggesting that for the identification of highly nonlinear systems, the simulation approach is the preferred one. Although the response of the system is slightly nonstationary, the proposed approach still gives good results.

Figs. 10 and 11 show contours of the conditional updated PDF $p(k_1, x_y|\hat{\mathbf{S}}^K_{y,N}, \hat{\sigma}_x, \hat{\sigma}_{\eta o})$ and $p(x_y, S_{fo}|\hat{\mathbf{S}}^K_{y,N}, \hat{k}_1, \hat{\sigma}_{\eta o})$, respectively, with all the other parameters fixed at their optimal values. It can be seen that the optimal parameter set is within two standard deviations away from the actual parameter set in both the (k_1, x_y) and (x_y, S_{fo}) planes, whereas this was not the case in the (x_y, σ_x) plane when the theoretical spectrum was estimated by equivalent linearization (see Fig. 9).

Example 3: Four-Story Inelastic Structure, White-Noise Excitation

The third example uses simulated response data for a four-story inelastic shear building shown in Fig. 12. The nonlinear springs have the same inelastic behavior as described in Fig. 5 in Example 2. The structure has uniformly distributed floor mass $m_j = 160$ ton, $j = 1, \ldots, 4$, and uniformly distributed story stiffness over its height. The linear stiffness to mass ratios $\tilde{k}_j/m_j$, $j = 1, \ldots, 4$, are chosen to be 1,310 s^{-2} so that the small-amplitude fundamental frequency is 2.00 Hz. Furthermore, the

Table 4. Identification Results for Four-Story Inelastic Shear Building with White-Noise Excitation (Example 3)

Parameter	Actual $\tilde{a}$	Optimal $\hat{a}$	Standard deviation σ	COV $\alpha=\frac{\sigma}{\tilde{a}}$	$\beta=\frac{\lvert\tilde{a}-\hat{a}\rvert}{\sigma}$
θ_1	1.0000	1.0122	0.0097	0.010	1.26
θ_2	1.0000	0.9907	0.0089	0.009	1.04
θ_3	1.0000	0.9903	0.0103	0.010	0.95
θ_4	1.0000	0.9947	0.0078	0.008	0.69
θ_y	1.0000	0.9577	0.0533	0.053	0.79
S_{fo}	0.0060	0.0076	0.0008	0.132	2.03
$\sigma_{\eta 1}$	0.0022	0.0022	0.0001	0.047	0.03
$\sigma_{\eta 2}$	0.0063	0.0062	0.0002	0.040	0.41

yielding level is chosen to be $\tilde{x}_y=0.015$ m for each story, which corresponds to 0.5% drift if the story height is 3.0 m. For better scaling in the identification process, the stiffness and yielding parameters are parameterized by: $k_j=\theta_j\hat{k}_j$, $j=1,\ldots,4$, and $x_y=\theta_y\tilde{x}_y$, where $\tilde{k}_j=2.10\times10^5$ kN/m and $\tilde{x}_y=0.015$ m are the nominal values for the linear stiffness of the jth story and the nominal yielding level for all four stories. The structure is assumed to be subjected to a white-noise base acceleration f with spectral intensity $S_{f0}=0.006\ \mathrm{m^2\,s^{-3}}$. Note that the matrix $\mathbf{T}$ in Eq. (14) is equal to the 4×1 matrix $-[m_1,m_2,m_3,m_4]^T$ in this case. Therefore, the model parameter vector for identification is $\mathbf{a}=[\theta_1,\theta_2,\theta_3,\theta_4,\theta_y,S_{f0},\sigma_{\eta1},\sigma_{\eta2}]^T$

To simulate noisy data, displacements at the second and fifth floors, i.e., at x_1 and x_4, were generated over a time interval $T=25$ s, using the exact parameter values $\tilde{\mathbf{a}}$. A sampling interval $\Delta t=0.01$ s was used, so the total number of measured time points is $N=2{,}500$. The noise added to the simulated response had a noise-to-signal ratio of 10%, i.e., the rms of the noise for a particular data channel is equal to 10% of the rms of the noise-free response at the corresponding DOF.

Fig. 13 shows the simulated noisy displacement time histories at x_1 and x_4, and Fig. 14 shows the hysteresis loops for the fourth story, that is, the restoring force $f_{s4}(t)$ normalized by m_4 versus the interstory displacement $x_4(t)-x_3(t)$. Note that these hysteresis loops are not assumed to be measured; they are shown only for the purpose of illustrating the level of nonlinearity. Note also that the nonlinearity in the other stories is even higher. The time histories were separated into five segments ($M=5$) with equal length in order to average five sets of spectral estimates. Recall that the expected value of the spectral density matrix estimator, $E[\mathbf{S}_{y,N}|\mathbf{a}]$, is obtained by the following procedure. First, simulate 100 system responses for the model parameters $\mathbf{a}$. Then, by using Eqs. (18) and (19), 100 samples of the spectral estimates can be obtained. By averaging these 100 samples for each discrete frequency, one obtains an estimate of the expected spectrum $E[\mathbf{S}_{y,N}|\mathbf{a}]$.

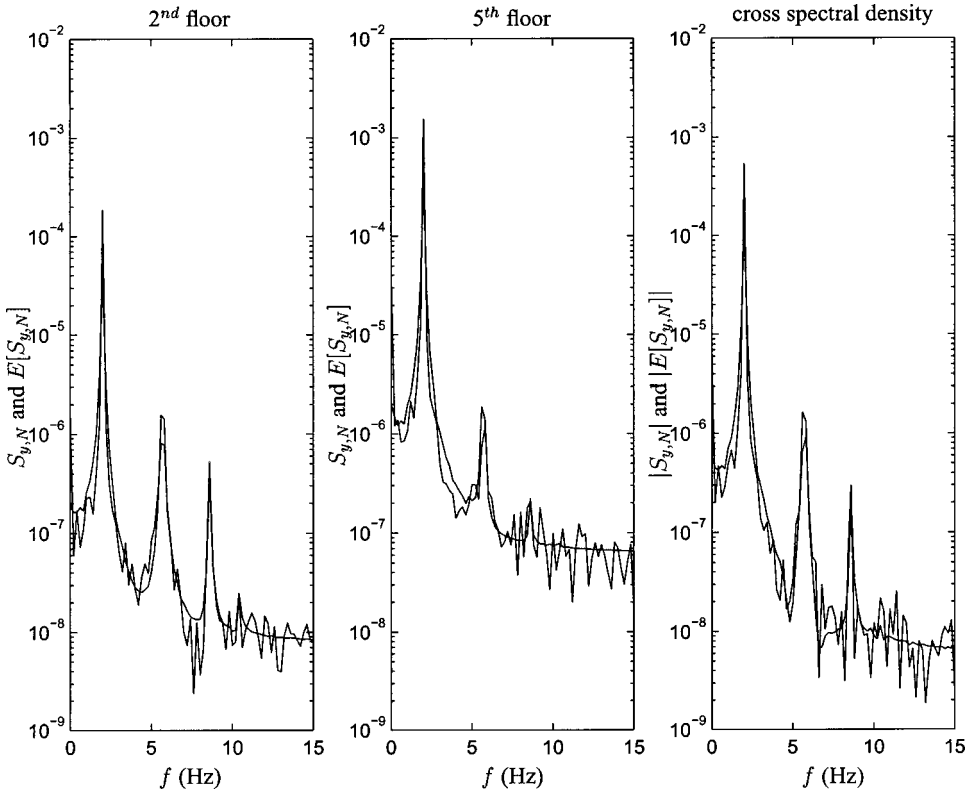

Fig. 15. Autospectral and cross-spectral estimates (zigzag) and their expected values (smooth) (Example 3)

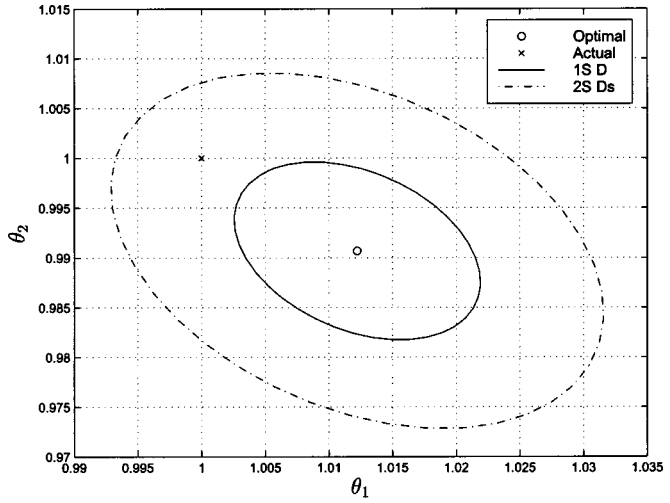

Fig. 16. Contours of conditional updated probability density function in (θ_1,θ_2) plane, keeping all other parameters at their optimal values (Example 3)

Table 4 shows the identification results utilizing the spectral estimates up to $\omega_K=16.0$ Hz ($K=80$). Again, a noninformative prior distribution for the model parameters is used. The second column in Table 4 corresponds to the actual values used for generation of the simulated measurement data; the third and fourth columns correspond to the identified optimal parameters and the corresponding standard deviations, respectively; the fifth column lists the coefficient of variation for each parameter; and the last column shows the normalized error β, which is the difference between the actual and optimal parameters normalized by the calculated standard deviation. The first group of rows in the table corresponds to the stiffness parameters θ_j, $j=1,\ldots,4$, followed by the yielding parameter θ_y, the forcing spectral intensity S_{f0} and the standard deviations of the prediction error, $\sigma_{\eta j}$, $j=1,2$, for the noise in the measured floor displacements, x_1 and x_4. As shown by the small COVs, all the parameter values are pinned down rather precisely by the data. Also, the normalized errors β are the order of 2 or less, suggesting that the procedure is not producing biased estimates.

Fig. 15 compares, for x_1 and x_4, the average autospectral estimates and the amplitude of the average cross-spectral estimates in $\hat{S}_{y,N}^M$ (zigzag curves) that are calculated from the $M=5$ equal-length time segments of data, with the corresponding expected values in $E[S_{y,N}|\hat{\mathbf{a}}]$ (smooth curves) for the optimal parameter estimates. One can see that the identified expected spectral densities fit all the peaks of the corresponding spectral densities estimated from the measurements for both floors.

Fig. 16 shows the contours in the (θ_1,θ_2) plane of the conditional updated PDF of θ_1 and θ_2 (keeping all other parameters fixed at their optimal values). One observes that the actual parameters are at a reasonable distance, measured in terms of the estimated standard deviations, from the identified optimal parameters.

Example 4: Four-Story Inelastic Structure, Nonwhite Excitation

In this example, the same structure as in Example 3 is subjected to nonwhite excitation given by filtered white noise with the Kanai–Tajimi spectrum (Clough and Penzien 1975):

$$S_{\ddot{x}_g\ddot{x}_g}=S_{f0}\frac{4\zeta_g^2\omega_g^2\omega^2+\omega_g^4}{(\omega^2-\omega_g^2)^2+4\zeta_g^2\omega_g^2\omega^2} \tag{36}$$

where the filter parameters are chosen as $\omega_g=5\pi$ rad/sec and $\zeta_g=0.5$. Identification is repeated under the same conditions as the previous case, except that the white-noise excitation is filtered by the Kanai–Tajimi filter before applying it to the structure. Note that the parameter vector a now also includes ω_g and ζ_g in addition to the eight parameters in Example 3.

Table 5 shows the identification results utilizing the spectral estimates up to $\omega_K=16.0$ Hz ($K=80$). Again, a noninformative prior distribution for the model parameters is used. The proposed method can successfully identify the structural parameters and the excitation parameters.

Conclusion

A Bayesian system identification approach was extended for updating the PDF of the model parameters for nonlinear systems using noisy response data only. The proposed spectral-based approach relies on the robustness of the Gaussian approximation for the FFT with respect to the probability distribution of the response signal in order to calculate the updated probability density function for the parameters of a nonlinear model conditional on the measured response. It does not require huge amounts of dynamic data, which is in contrast to most other published system identification methods for nonlinear models and unknown input. The approach provides not only the optimal estimates of the parameters but also the relative plausibilities of all values of the

Table 5. Identification Results for Four-Story Inelastic Shear Building with Nonwhite Excitation (Example 4)

Parameter	Actual $\tilde{a}$	Optimal $\hat{a}$	Standard deviation σ	COV $\alpha=\frac{\sigma}{\tilde{a}}$	$\beta=\frac{\lvert\tilde{a}-\hat{a}\rvert}{\sigma}$
θ_1	1.0000	1.0029	0.0142	0.014	0.20
θ_2	1.0000	0.9792	0.0170	0.017	1.22
θ_3	1.0000	0.9962	0.0210	0.021	0.18
θ_4	1.0000	1.0469	0.0241	0.024	1.95
θ_y	1.0000	0.9547	0.0303	0.030	1.51
S_{fo}	0.0060	0.0074	0.0008	0.133	1.75
$\sigma_{\eta 1}$	0.0027	0.0032	0.0003	0.111	1.67
$\sigma_{\eta 2}$	0.0081	0.0077	0.0005	0.062	0.80
ω_g	15.708	15.910	0.1123	0.007	1.80
ζ_g	0.5000	0.5737	0.0296	0.059	2.49

parameters based on the data. This probabilistic description is very important and can avoid misleading results, especially in unidentifiable cases. For the examples presented, the updated PDFs for the model parameters are well approximated by a multivariate Gaussian distribution and so the precision with which the parameters are specified by the system response data are readily calculated.

References

Beck, J. L. (1990). ''Statistical system identification of structures.'' *Structural Safety and Reliability*, ASCE, New York, 1395–1402.

Beck, J. L., and Au, S. K. (2002). ''Bayesian updating of structural models and reliability using Markov Chain Monte Carlo simulation.'' *J. Eng. Mech.*, 128(4), 380–391.

Beck, J. L., and Katafygiotis, L. S. (1998). ''Updating models and their uncertainties. I: Bayesian statistical framework.'' *J. Eng. Mech.*, 124(4), 455–461.

Beck, J. L., May, B. S., and Polidori, D. C. (1994). ''Determination of modal parameters from ambient vibration data for structural health monitoring.'' *Proc., 1st World Conf. on Structural Control*, Pasadena, Calif., TA3:3–TA3:12, International Association of Structural Control.

Box, G. E. P., and Tiao, G. C. (1973). *Bayesian Inference in Statistical Analysis*. Addison-Wesley, Reading, Mass.

Brillinger, D. R. (1969). ''Asymptotic properties of spectral estimates of second order.'' *Biometrika*, 56(2), 375–390.

Clough, R. W., and Penzien, J. (1975). *Dynamics of structures*, McGraw-Hill, New York.

Gersch, W., Taoka, G. T., and Liu, R. (1976). ''Structural system parameter estimation by two-stage least squares method.'' *J. Eng. Mech.*, 102(5), 883–899.

Hoshiya, M., and Saito, E. (1984). ''Structural identification by extended Kalman filter.'' *J. Eng. Mech.*, 110(12), 1757–1770.

Housner, G. W., Bergman, L. A., Caughey, T. K., Chassiakos, A. G., Claus, R. O., Masri, S. F., Skelton, R. E., Soong, T. T., Spencer, B. F., and Yao, J. T. P. (1997). ''Special issue on structural control: past, present, and future.'' *J. Eng. Mech.*, 123(9).

Iwan, W. D., and Lutes, L. D. (1968). ''Response of the bilinear hysteretic system to stationary random excitation.'' *J. Acoust. Soc. Am.*, 43, 545–552.

Katafygiotis, L. S., Papadimitriou, C., and Lam, H. F. (1998). ''A probabilistic approach to structural model updating.'' *Soil Dyn. Earthquake Eng.*, 17(7–8), 495–507.

Katafygiotis, L. S., and Yuen, K.-V. (2001). ''Bayesian spectral density approach for modal updating using ambient data.'' *Earthquake Eng. Struct. Dyn.*, 30(8), 1103–1123.

Krishnaiah, P. R. (1976). ''Some recent developments on complex multivariate distributions.'' *J. Multivariate Anal.*, 6, 1–30.

Loh, C.-H., and Tsaur, Y.-H. (1988). ''Time domain estimation of structural parameters.'' *Eng. Struct.*, 10(2), 95–105.

Lutes, L. D., and Sarkani, S. (1997). *Stochastic analysis of structural and mechanical vibrations*, Prentice Hall, Englewood Cliffs, N.J.

MATLAB (1994). *Matlab user's guide*, MathWorks, Inc., Natick, Mass.

Natke, H. G., and Yao, J. T. P. (1988). *Proc., Workshop on Structural Safety Evaluation Based on System Identification Approaches*, Vieweg and Sons, Wiesbaden.

Roberts, J. B., Dunne, J. F., and Debonos, A. (1995). ''A spectral method for estimation for nonlinear system parameters from measured response.'' *Probab. Eng. Mech.*, 10(4), 199–207.

Roberts, J. B., and Spanos, P. D. (1990). *Random vibration and statistical linearization*, Wiley, New York.

Vanik, M. W., Beck, J. L., and Au, S. K. (2000). ''A Bayesian probabilistic approach to structural health monitoring.'' *J. Eng. Mech.*, 126(7), 738–745.

Yaglom, A. M. (1987). *Correlation theory of stationary and related random functions*. Springer, New York.

Yajima, Y. (1989). ''A central limit theorem of fourier transforms of strongly dependent stationary processes.'' *J. Time Ser. Anal.*, 10(4), 375–383.

Yuen, K.-V. (1999). ''Structural modal identification using ambient dynamic data.'' MPhil thesis, Tech. Rep., Hong Kong Univ. of Science and Technology, Hong Kong.

Yuen, K.-V., Beck, J. L., and Katafygiotis, L. S. (2002). ''Probabilistic approach for modal identification using non-stationary noisy response measurements only.'' *Earthquake Eng. Struct. Dyn.*, 31(4), 1007–1023.

Yuen, K.-V., and Katafygiotis, L. S. (2001). ''Bayesian time-domain approach for modal updating using ambient data.'' *Probab. Eng. Mech.*, 16(3), 219–231.

Yuen, K.-V., and Katafygiotis, L. S. (2002). ''Bayesian modal updating using complete input and incomplete response noisy measurements.'' *J. Eng. Mech.*, 128(3), 340–350.

Yuen, K.-V., Katafygiotis, L. S., and Beck, J. L. (2002). ''Spectral density estimation of stochastic vector processes.'' *Probab. Eng. Mech.*, 17(3), 265–272.

Zeldin, B. A., and Spanos, P. D. (1998). ''Spectral identification of nonlinear structural systems.'' *J. Eng. Mech.*, 124(7), 728–733.